Chinese Journal of Oceanology and Limnology
Vol. 34 No. 5, P. 902-914, 2016
http://dx.doi.org/10.1007/s00343-016-4202-6

Distribution patterns of phytoplankton in the Changjiang River estuary and adjacent waters in spring 2009*

KONG Fanzhou (孔凡洲)[1, 2], XU Zijun (徐子钧)[3], YU Rencheng (于仁成)[1, 2, **],
YUAN Yongquan (袁涌铨)[1, 2], ZHOU Mingjiang (周名江)[1]

[1] *Key Laboratory of Marine Ecology and Environmental Sciences*, *Chinese Academy of Sciences*, *Qingdao 266071*, *China*

[2] *Laboratory of Marine Ecology and Environmental Science*, *Qingdao National Laboratory for Marine Science and Technology*, *Qingdao 266071*, *China*

[3] *North China Sea Monitoring Centre*, *Qingdao 266033*, *China*

Received Aug. 1, 2014; accepted in principle Oct. 2, 2014; accepted for publication Jul. 14, 2015
© Chinese Society for Oceanology and Limnology, Science Press, and Springer-Verlag Berlin Heidelberg 2016

Abstract The Changjiang River estuary and adjacent waters are one of the most notable regions for red tides/harmful algal blooms in China's coastal waters. In this study, phytoplankton samples were collected and analyzed during the outbreak stage of red tides in May 2009. It was found that dinoflagellates, *Prorocentrum donghaiense* and *Karenia mikimotoi*, and diatoms, *Skeletonema* spp. and *Paralia sulcata*, were the major taxa dominating the phytoplankton community. Cluster analysis, non-metric multidimensional scaling (NMDS) and analysis of similarities (ANOSIM) was conducted on a data matrix including taxa composition and cell abundance of the phytoplankton samples. The analyses categorized the samples into three groups at a similarity level of 30%. Group I was characterized by estuarine diatoms and distributed mainly in the highly turbid estuarine region. Group II, which was dominated by the diatom *Skeletonema* spp. and represented the red tide of *Skeletonema* spp., was situated around Group I in the sea area west of 122°50′E. Group III was characterized by a high proportion of dinoflagellates and was found further offshore compared with Groups I and II. Group III was further divided into two subgroups (III-S1 and III-S2) at a similarity level of 40%. Group III-S1 was characterized by the presence of the benthic diatom *P. sulcata*, representing phytoplankton samples collected either from the bottom or from the sea area affected by upwelling. Group III-S2 was dominated by dinoflagellates and represented red tides formed by *P. donghaiense* and *K. mikimotoi*. A gradual change of red-tide causative species was observed from the estuary to the offshore sea area, from diatoms to armored dinoflagellates and then unarmored dinoflagellates. Environmental factors associated with each group, and thus affecting the distribution of phytoplankton and red tides, are discussed.

Keyword: phytoplankton; cluster analysis; red tide; distribution; Changjiang River estuary

1 INTRODUCTION

The Changjiang (Yangtze) River is the longest river in China, with a drainage area of 1.8 million km^2. Large quantities of nutrients are transported into the sea through the Changjiang River, and this area forms an important basis for the Zhoushan fishing ground. However, the quantity of nutrients discharged into the estuary and its adjacent waters has significantly increased with the rapid development of industry and agriculture in the drainage basin of the Changjiang River, and resulted in the serious problems with eutrophication and red tides (Wang et al., 2002; Wang, 2007; Pei et al., 2009). A red tide is the abnormal phenomenon of seawater discoloration caused by excessive growth or accumulation of microscopic plankton. Some red tides, generally termed as harmful algal blooms, bring deleterious impacts on marine organisms and ecosystems, and subsequently human

* Supported by the Youth Program of the National Natural Science Foundation of China (No. 41206098), the Strategic Priority Research Program of the Chinese Academy of Science (No. XDA11020304), the Fund for Creative Research Groups of NSFC (No. 41121064), the joint program supported by the NSFC and Shandong Province (No. U1406403), and the Open Foundation of the Shandong Provincial Key Laboratory of Marine Ecology and Environment & Disaster Prevention and Mitigation (No. 2011006)
** Corresponding author: rcyu@qdio.ac.cn

health (GEOHAB, 2001).

The Changjiang River estuary (CRE) and adjacent waters are among the most notable regions for red tides in the coastal waters of China. Large scale red tides of *Prorocentrum donghaiense* have been recorded every spring in the coastal waters adjacent to the CRE since 2000, and the maximum affected sea area is, at times, over 10 000 km^2 (Zhou and Yu, 2007). Red tides were mainly found in the sea area with abrupt changes in bottom topography at depths of 30–50 m (Zhou et al., 2003; Tang et al., 2006). In the spring, red tides of both diatoms and dinoflagellates were found in this region, and there was an apparent succession of red tide causative species from diatoms to dinoflagellates from March to May (Zhou et al., 2008). With increasing water temperature and light intensity, diatoms take advantage of the nutrients accumulated over the winter and grow rapidly to form the first red tides. Once nutrients, particularly phosphate, are consumed to a low level, and thus the growth of diatoms is limited, the diatom red tide will reduce in size. Subsequently, with the continuous increase in water temperature and the occurrence of stratification, red tides of dinoflagellates appear (Zhou and Zhu, 2006). There is a high frequency of red tides and other abnormal ecological events, such as jellyfish blooms and hypoxia, occurring in the sea area adjacent to the CRE. This has caused this region to become a hot spot in marine ecological studies in China since the beginning of the new millennium (Shen and Hong, 1994; Huang et al., 2000; Wang and Huang, 2003).

Many investigations have been performed in the CRE and its adjacent waters during the last few decades because of the ecological significance of this region. In phytoplankton ecological studies conducted prior to the appearance of massive dinoflagellate red tides in this region around the year 2000, most samples were collected with a phytoplankton net (nominal pore size at 67 μm) (Wu et al., 2000). Those net-concentrated samples, however, are not suitable for studies of dinoflagellate red tides, because the bloom-forming species like *P. donghaiense*, *Karenia mikimotoi*, *Gyrodinium spirale*, *Scrippsiella trochoidea* and *Alexandrium* spp. in the CRE and adjacent waters are generally less than 70 μm in cell size. Additionally, there is no information on the vertical distribution of red tides using net-concentrated samples. Therefore, the collection of discrete water samples are gradually accepted in phytoplankton investigations (Gao and Song, 2005; Chen et al., 2006; Luan et al., 2006; He et al., 2009; Zhao et al., 2010; Sun and Tian, 2011) and red tide studies in the CRE and adjacent waters.

To understand the phytoplankton distribution patterns, statistical methods like cluster analysis are often adopted. Cluster analysis has been widely used in marine ecological studies of planktonic and benthic communities. This method was used to analyze net-concentrated phytoplankton samples in the CRE and adjacent waters, and the phytoplankton assemblage was classified into "freshwater community", "estuary community" and "offshore community" (Guo and Yang, 1992; Wu et al., 2000; Wang, 2002). However, the application of such methods to analyze discrete water samples of phytoplankton in the sea area adjacent to the CRE is still quite limited (Zhao et al., 2010).

A comprehensive survey was carried out from 7 to 18 May in 2009 in the CRE and adjacent waters (30°30′–32°00′N, 122°00′–123°20′E). Discrete water samples were collected during the cruise, and phytoplankton taxa and abundance were determined by microscope. Cluster analysis and non-metric multidimensional scaling (NMDS) were conducted on a data matrix that included taxa composition and cell abundance of the phytoplankton samples. The purpose of this study was to reveal the distribution patterns of phytoplankton, and their relationship with environmental factors in the CRE and adjacent waters.

2 MATERIAL AND METHOD

2.1 Study area

The study area, located in the CRE and adjacent coastal waters (30°30′–32°00′N, 122°00′–123°20′E), is illustrated in Fig.1. The average depth of the study area was about 30 m, and the sea bottom topography was characterized by a sharp gradient between longitudes 122°30′E and 123°00′E (water depth 20–60 m). This area is significantly affected by freshwater discharge from the Changjiang River as well as seasonal upwelling, resulting in a rich biodiversity of phytoplankton. Large quantities of nutrients transported into this area by the Changjiang River make this a highly productive region. The over-enrichment of nutrients, however, has caused this region the most notable red tide zone in the coastal waters of China after the year 2000.

2.2 Sample collection

Phytoplankton samples (n=72) were collected from

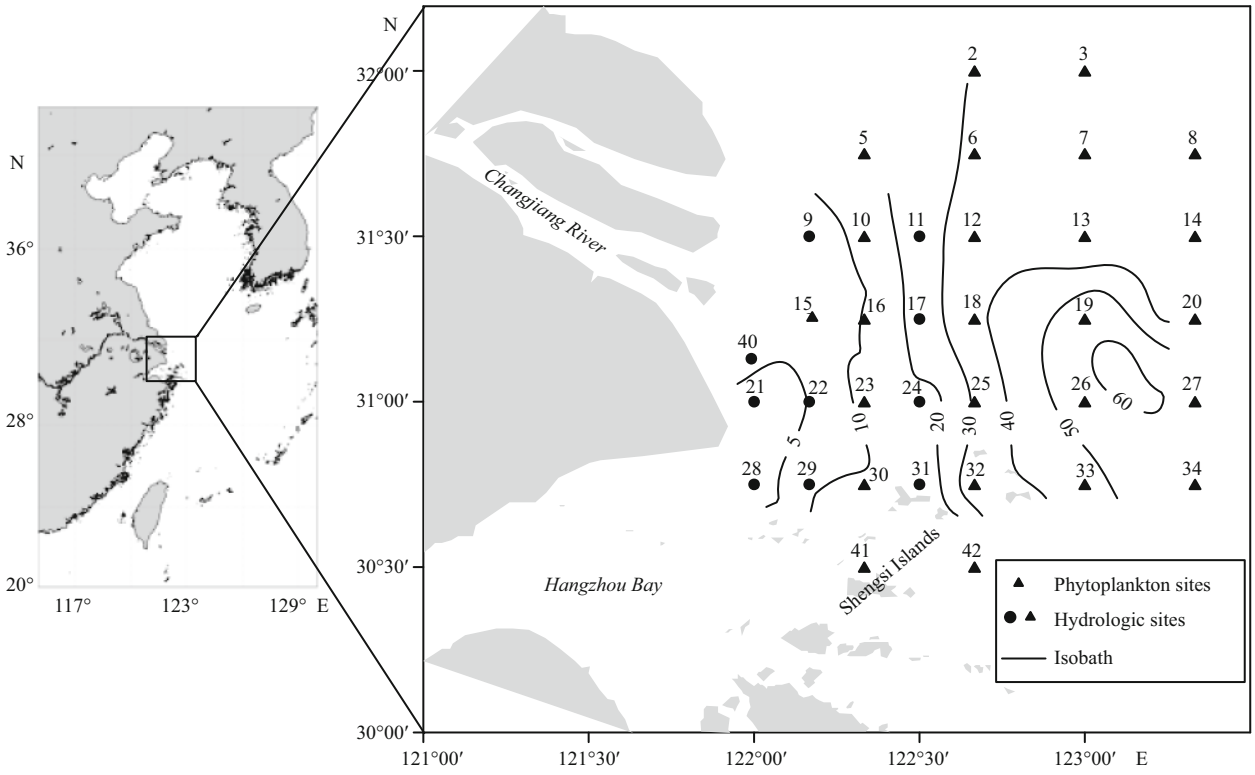

Fig.1 Study area and sampling sites

Depth contours of the study area are marked in grey lines.

the surface and at different depths (10 m, 30 m, and in the bottom layer about 2 m above seafloor), using water samplers installed on an ALEC CTD (JFE Advantech Co. Ltd., Nishinomiya, Japan) at 24 sampling sites. The water samples (0.5 L) were fixed with 6–8 mL Lugol's solution and stored at room temperature. Concentrating phytoplankton in water samples was achieved using Utermöl's methods (Utermöhl, 1958). Briefly, 25 mL well-mixed water sample was placed into a sedimentation chamber and settled for 24 h (Lund et al., 1958). The microalgae were then identified and counted under an inverted microscope.

To accurately depict the complex hydrological conditions, hydrological variables, such as seawater temperature, salinity and turbidity (NTU), were obtained from the 34 sampling sites (Fig.1) using the ALEC CTD. Measurements were made at the same depths as the collection of water samples and at additional depths at 5 m and 20 m.

2.3 Data analysis

2.3.1 Biodiversity indices

The Margalef index (d_{Ma}) (Margalef, 1958), Shannon index (H) (Shannon, 1948), Pielou evenness index (J) (Pielou, 1966) and dominance index (Y_i) (McNaughton, 1967) were used to represent the biodiversity of the phytoplankton community. The Margalef index (d_{Ma}) reflects species richness using the number of phytoplankton species and the abundance of phytoplankton. The Shannon index (H) is used to measure the species biodiversity of a sample. The Pielou evenness index (J) indicates the species distribution evenness in the community. The dominance index (Y_i) helped to determine the dominant species, and excluded interference of rare species for data analysis. Indices d_{Ma}, H and J were calculated with Biodixcel.xlsx (Kong et al., 2012), with the following formulae:

$$d_{\mathrm{Ma}} = \frac{(S-1)}{\ln N}, \tag{1}$$

$$H = -\sum_{i=1}^{S} P_i \log_2 P_i, \tag{2}$$

$$J = \frac{H}{\log_2 S}, \tag{3}$$

$$Y_i = \frac{n_i}{N} f_i, \tag{4}$$

where S is the total number of phytoplankton species,

N is the abundance of phytoplankton, P_i is the proportion of individuals belonging to the i^{th} species in the dataset of interest, n_i is the abundance of the i^{th} species, and f_i is the frequency of the i^{th} species occurring in the samples.

2.3.2 Cluster analysis and non-metric multi-dimensional scaling

Data analysis was conducted on a data matrix that included both taxa composition and cell abundance in the 72 phytoplankton samples collected from 24 sites. Rare species with a frequency below 10% were not taken into consideration. A standardized triangle similarity matrix was constructed through the Bray-Curtis similarity measure, and fourth root transformation analysis was adopted to balance rare and common species. Based on Bray-Curtis similarities, hierarchical clustering with group-average linking was constructed. However, cluster analysis itself, which shows the similarities of the samples in the same group in one-dimensional quality level, is not enough to reflect the characteristics of the whole community. Therefore, cluster analysis was used in conjunction with NMDS and analysis of similarity (ANOSIM) methods. The samples were ordinated by NMDS in a two-dimensional map. The stress coefficient (s) of the ordination, in the case of NMDS, indicates excellent representation (s<0.05), adequate ordination (s<0.2) or arbitrary ordination (s>0.3) (Clarke and Warwick, 2001). ANOSIM analysis was used to test the significance of difference among the clusters, and SIMPER analysis was used to compare average abundance and examine the contribution of each species to similarities within a given group, or dissimilarities between groups (Clarke and Warwick, 2001). The above analyses were performed with PRIMER 6.0 software (Clarke and Gorley, 2006). To prepare the contour maps for cell abundance and different hydrological variables, Surfer 11 was used with the Kriging gridding method.

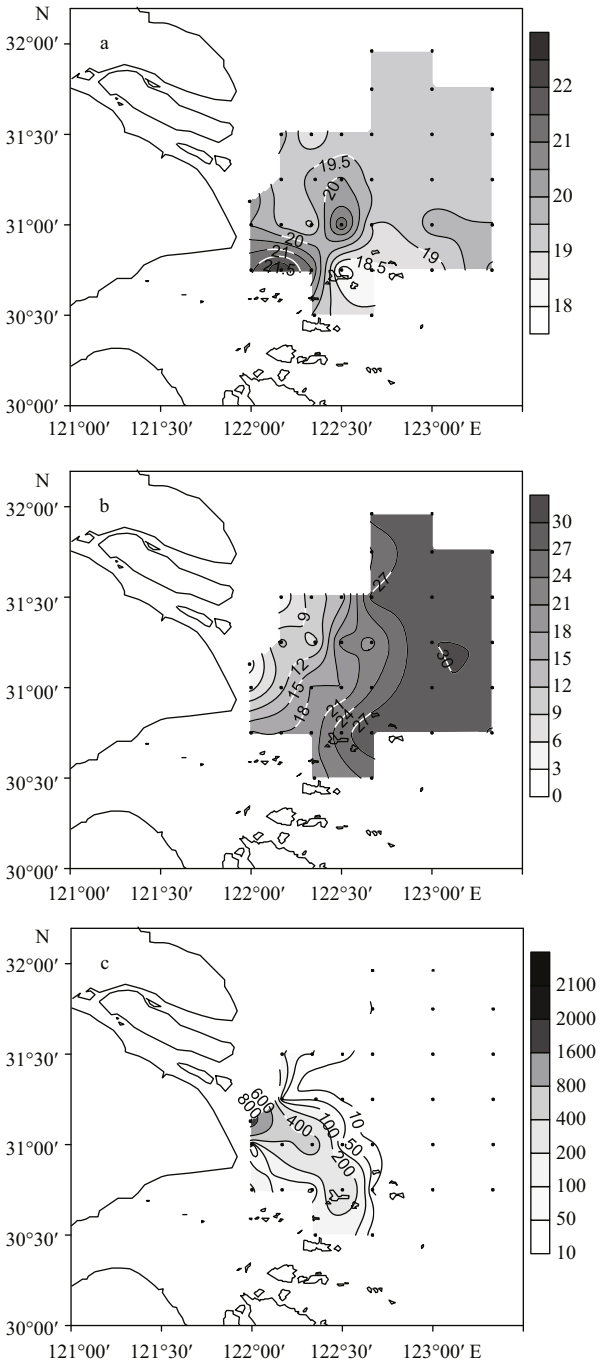

Fig.2 Horizontal distribution of temperature (a), salinity (b) and turbidity (c) at the surface in the study area

3 RESULT

3.1 Hydrological conditions at the study area

The water temperature, salinity and turbidity in the study area are illustrated in Fig.2. Water temperature at the surface ranged from 18.4–21.1°C, while for most of the sampling sites, water temperature was between 19.0–19.5°C. Water temperature was generally higher in the southern part of the study area than in the northern part (Fig.2a). However, there was an obvious low-temperature area around sampling site 32 in the southern part of the study area.

Salinity in the study area ranged from 7.9–30.06. Salinity increased gradually from the estuary to the offshore area, forming a bifurcation near sampling site 15, and an area with dense isohalines along the longitude 122°30′E (Fig.2b).

Turbidity in the study area ranged from 0–1820 NTU. The diluted water at the southern branch from

Table 1 Arithmetic mean and range (minimum-maximum) of temperature, salinity and turbidity at different sampling depths in the study area

Sampling depth	Temperature (°C)	Salinity	Turbidity (NTU)
Surface	19.3 (18.4–21.1)	24.3 (7.9–30.1)	39.7 (0–536.5)
10 m	18.4 (16.8–19.8)	29.9 (28.2–32.5)	5.0 (0–53.0)
30 m	17.2 (16.6–17.8)	33.0 (32.0–33.5)	9.3 (0–33.8)
Bottom	17.2 (16.4–19.9)	30.6 (18.4–33.5)	202.2 (0–1 820.2)

Table 2 Dominant phytoplankton taxa in the study area

Species	Distribution frequency (f_i)	Dominance (Y)
Prorocentrum donghaiense	0.777 8	0.401 5
Skeletonema spp.	0.361 1	0.166 1
Karenia mikimotoi	0.250 0	0.004 7
Paralia sulcata	0.416 7	0.000 4
Thalassiosira spp.	0.763 9	0.000 3
Gyrodinium spirale	0.458 3	0.000 2

the bifurcation point had much higher turbidity and affected a large sea area. The high turbidity area was distributed mainly at the entrance of the CRE (Fig.2c), the entrance of Hangzhou Bay and the area around the Shengsi Islands. Turbidity in the sea area east of latitude 122.4°E decreased rapidly to below 10 NTU.

Temperature, salinity and turbidity at different sampling depths are shown in Table 1. Obvious halocline and thermocline layers could be observed. The temperature was about 2°C higher at the surface than at the bottom, while salinity at the surface was much lower than the bottom, reflecting stratification under the influence of the Changjiang River diluted water.

3.2 Dominant species in the phytoplankton samples

In the 72 phytoplankton samples, 94 taxa were identified, including 52 taxa of diatoms, 40 taxa of dinoflagellates, and two species of chrysophytes. Diatoms and dinoflagellates dominated the phytoplankton assemblage in the CRE and adjacent coastal waters.

Dominant microalgae, defined by a dominance index Y_i higher than 0.000 2, are listed in Table 2. The dominant phytoplankton taxa were, in descending order, *P. donghaiense*, *Skeletonema* spp., *K. mikimotoi*, *Paralia sulcata*, *Thalassiosira* spp. and *Gyrodinium spirale*.

3.3 Abundance and distribution of major phytoplankton groups

Average phytoplankton abundance in the study area was 46.0 (0.012–883.8)×10^4 cells/L. The abundance of diatoms and dinoflagellates was 21.26 (0–883)×10^4 cells/L and 24.7 (0–351)×10^4 cells/L, respectively, accounting for 46%(0–100%) and 53.7% (0–92%) of the total abundance of phytoplankton. In the surface seawater, phytoplankton abundance was 85.8 (0.05–883)×10^4 cells/L, while the abundances of diatoms and dinoflagellates were 47.3 (0–883)×10^4 cells/L and 38.5 (0–350)×10^4 cells/L, respectively. With respect to the dominant taxa, the abundances of *P. donghaiense*, *Skeletonema* spp. and *K. mikimotoi* were 36.8 (0–350), 47.1 (0–883) and 1.5 (0–35)×10^4 cells/L, respectively.

The distributions of major phytoplankton groups and dominant microalgal taxa at the surface are shown in Fig.3. The horizontal distribution patterns of diatoms and dinoflagellates coincide well with their dominant species, *Skeletonema* spp. and *P. donghaiense*.

The vertical distribution of major phytoplankton groups and dominant taxa are listed in Table 3. The abundance of both dinoflagellates and diatoms decreased with water depth, and the minimum value of diatoms appeared at 30 m depth.

3.4 Analysis of the phytoplankton community

3.4.1 Classification of the phytoplankton community

According to the cluster analysis (Fig.4), phytoplankton samples collected from the study area could be divided into three major clusters (Group I–III) at a similarity level of 30%, except for 1 sample collected at a depth of 10 m from sampling site 42 (sample T42 on the left of the dendrogram). Group I included 16 samples evenly arranged in the dendrogram with a low similarity level. Group II included five samples with a similarity level of around 70%. Group III had 50 samples, which could be further divided into two subgroups (III-S1, III-S2) at a similarity level of 40%.

The non-metric multidimensional scaling map is shown in Fig.5. Except for sample T42, which could be distinguished from other samples at a similarity of 20%, the other samples were classified into three groups at a similarity level around 30%. Each group took up a fixed position, although there was an overlap between Groups I and III. The two groups might be

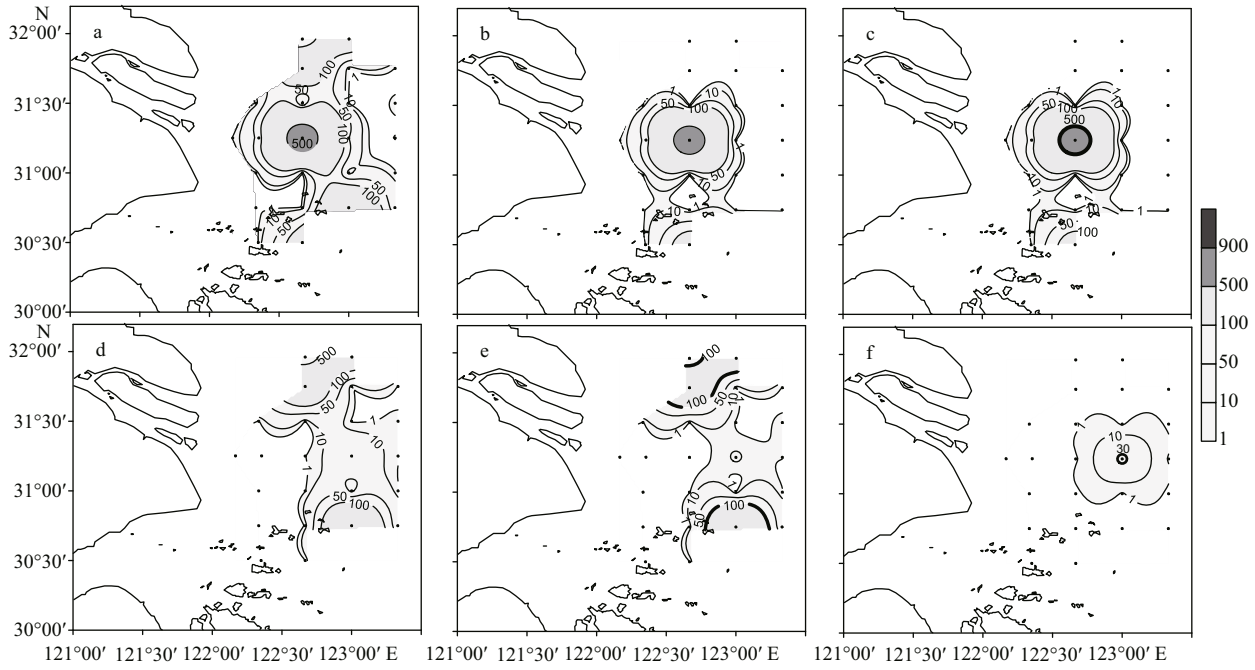

Fig.3 Distribution of major phytoplankton groups and dominant microalgal species at the surface in the study area (abundance, ×10⁴ cells/L)

a. total phytoplankton; b. diatoms; c. *Skeletonema* spp.; d. dinoflagellates; e. *Prorocentrum donghaiense*; and f. *Karenia mikimotoi*. Bold lines in (c), (e) and (f) indicate the distribution of red tides of *Skeletonema* spp., *Prorocentrum donghaiense* and *Karenia mikimotoi*.

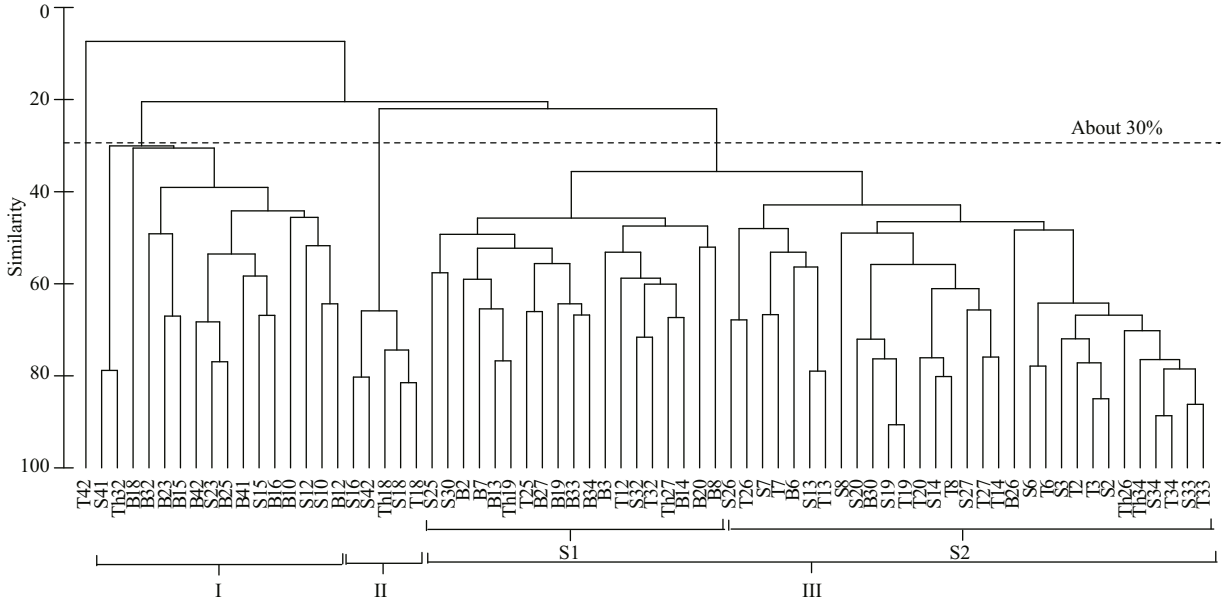

Fig.4 Clustering dendrogram of the phytoplankton community in the study area

Samples were named after the sampling site codes and the sampling depth, where "S" for surface, "T" for 10 m depth, "Th" for 30 m depth and "B" for bottom.

Table 3 Abundance of phytoplankton and dominant taxa at different depths

Sampling depth	Abundance (cells/L)						
	Phytoplankton	Dinoflagellates	Diatoms	*Prorocentrum donghaiense*	*Skeletonema* spp.	*Karenia mikimotoi*	*Paralia sulcata*
Surface	520–8.8×10⁶	0–3.5×10⁶	0–8.8×10⁶	0–3.5×10⁶	0–8.8×10⁶	0–3.5×10⁵	0–2 040
10 m	480–3.3×10⁶	80–2.2×10⁶	0–2.9×10⁶	0–2.2×10⁶	0–2.9×10⁶	0–1.7×10⁵	0–3 040
30 m	240–1.2×10⁶	0–5.7×10⁵	120–9.8×10⁵	0–5.7×10⁵	0–9.8×10⁵	0–240	0–560
Bottom	120–3.8×10⁵	0–3.8×10⁵	40–5 120	0–2.8×10⁵	0–1 080	0–9.2×10⁴	0–3 350

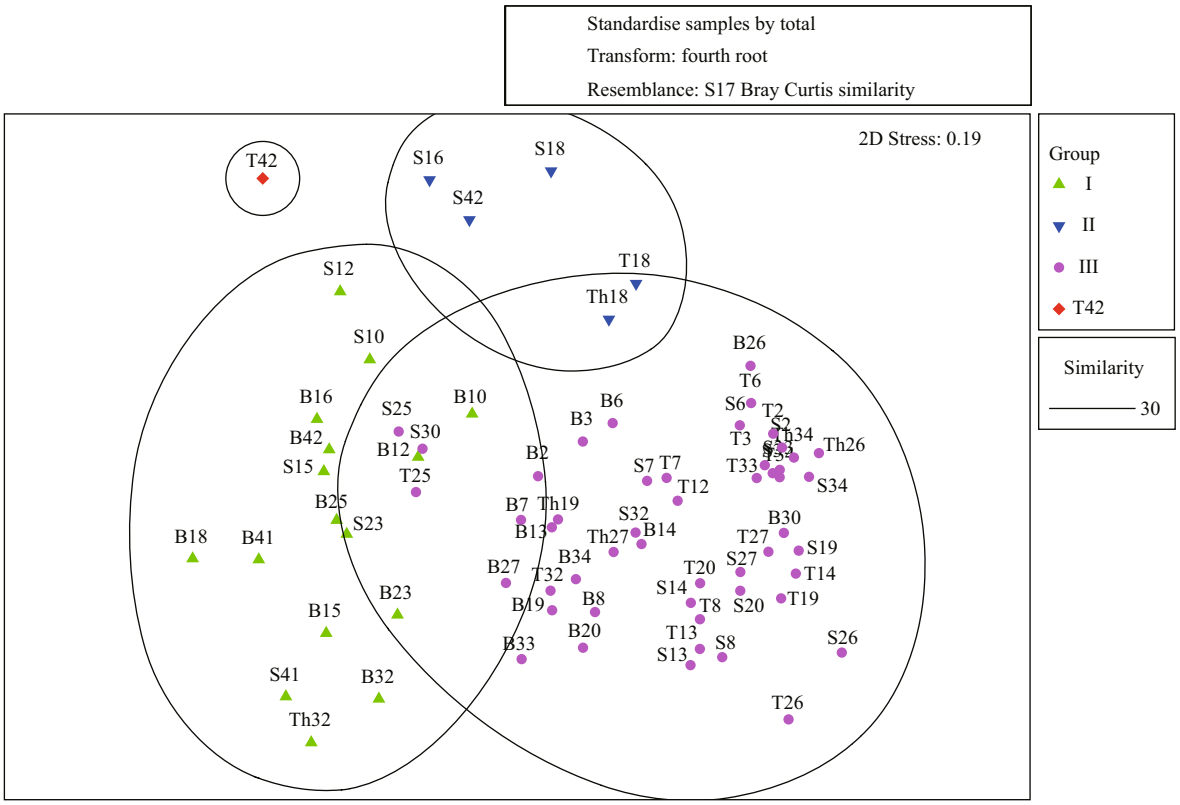

Fig.5 NMDS ordination of the phytoplankton communities in the study area

better distinguished in scaling analysis with more dimensions, but the 2-dimension scaling map was enough to demonstrate the similarity in each group of phytoplankton samples. The pressure coefficient (*s*) was 0.19, and therefore, the classification could reflect differences among the phytoplankton samples collected from the study area.

ANOSIM found significant differences among the groups (the value of global *R* was 0.749, $P<0.1\%$). Excluding sample T42, there were significant differences between any two selected groups ($P<0.1\%$) (Table 4), and therefore, the classification was credible.

3.4.2 Characterization of different phytoplankton groups

The dominant species, abundance, relative contribution of diatoms and dinoflagellates, and biodiversity indices for each group of phytoplankton samples are shown in Tables 5 and 6.

Among the three groups, Group I possessed the highest biodiversity, but the lowest abundance of phytoplankton. Phytoplankton samples in Group I were dominated by diatoms, and the dominant taxa were *Skeletonema* spp., *P. sulcata*, *Chaetoceros* spp., *Thalassiosira* spp., *Nitzschia* spp. and *Coscinodiscus* spp., with abundances of 1 847, 675, 282, 226, 118 and 104 cells/L, respectively. *Skeletonema* spp. accounted for around 50% of the total diatom cells.

Samples from Group II had the lowest biodiversity, and *Skeletonema* spp. dominated all phytoplankton samples. On average, the abundance of *Skeletonema* spp. was 3.2×10^6 cells/L, which accounted for 94% of the total phytoplankton cells. The abundance of dinoflagellate *P. donghaiense* was 1.2×10^5 cells/L, accounted for only 6% of the total phytoplankton cells. The abundance of other microalgal species was much lower compared with *Skeletonema* spp. and *P. donghaiense*. Those species with abundances higher than 100 cells/L were *P. sulcata*, *Thalassiosira* spp., *Melosira* sp. and *Prorocentrum minimum*.

The samples from Group III were characterized by a high proportion of dinoflagellates. This group was further divided into two subgroups. The phytoplankton abundances in the samples from subgroup III-S1 were relatively low (7 145 cells/L), and the dominant species were *P. donghaiense* and *P. sulcata*. The presence of the benthic diatom *Paralia sulcata* was the major characteristic of subgroup III-S1. Other taxa, including *Skeletonema* spp., *Thalassiosira* spp. and *S. trochoidea*, were also present in III-S1, with abundances of 341, 238 and 92 cells/L, respectively.

Table 4 Pair-wise ANOSIM test results between different groups

Groups	*R* statistic	*P* values (as significance level, %)	Possible permutations	Actual permutations	Number≥Observed
I, II	0.673	0.1	20349	999	0
I, III	0.734	0.1	Very large	999	0
I, T42	0.832	5.9	17	17	1
II, III	0.748	0.1	Very large	999	0
II, T42	1	16.7	6	6	1
III, T42	0.986	2	51	51	1

Table 5 The arithmetic mean and standard deviation of phytoplankton abundance in different groups

	Phytoplankton	Dinoflagellates	Diatoms	*Prorocentrum donghaiense*	*Skeletonema* spp.	*Karenia mikimotoi*	*Paraliasulcata*	*Thalassiosira* spp.
I	4 602±6 326	807±2 189	3 788±5 160	16±43	1 847±4 584	-	675±852	226±212
II	$(3.2±3.3)×10^6$	$(1.3±1.8)×10^5$	$(3.0±3.4)×10^6$	$(1.3±1.8)×10^5$	$(3.0±3.4)×10^6$	-	512±866	-
III	$(3.4±7.6)×10^5$	$(3.4±7.6)×10^5$	1 172±1 416	$(3.3±7.6)×10^5$	190±582	$(1.2±5.6)×10^4$	427±819	300±513
III-S1	7 148±8 337	5 164±7 980	1 984±1 540	4 772±7 794	341±818	21±59	1 124±999	61±91
III-S2	$(5.5±9.1)×10^5$	$(5.5±9.1)×10^5$	675±1 086	$(52±9.1)×10^5$	97±358	$(2.0±7.0)×10^4$	-	446±605
T42	480	80	400	-	-	-	-	-

Table 6 Comparison of species composition, abundance and biodiversity status among different groups

	Species number			Relative abundance (%)		Biodiversity index		
	Total	Diatoms	Dinoflagellates	Diatoms	Dinoflagellates	Pielou Index	Shannon Index	Margalef Index
I	11.59±5.50	9.53±4.82	1.94±2.38	86.85±14.13	13.03±14.08	0.20±0.08	2.25±0.79	1.32±0.62
II	7.60±2.97	3.60±1.34	4.00±3.54	93.83±8.68	6.17±8.68	0.01±0.02	0.26±0.34	0.45±0.19
III	11.38±3.95	4.36±2.65	7.00±3.41	19.42±26.59	80.56±26.58	0.11±0.09	1.29±0.93	1.07±0.42
III-S1	10.68±3.22	6.00±2.47	4.68±1.89	43.52±28.49	56.43±28.44	0.16±0.07	1.86±0.71	1.17±0.42
III-S2	11.81±4.33	3.35±2.24	8.42±3.37	4.65±8.60	95.35±8.60	0.08±0.08	0.94±0.88	1.01±0.41
T42	6	5	1	83.33	16.67	0.29	2.58	0.81

Samples in subgroup III-S2 were characterized by a high abundance of dinoflagellates. On average, phytoplankton abundance was $55.0×10^4$ cells/L, in which dinoflagellates accounted for more than 95%. *Prorocentrum donghaiense* was the dominant species, with an abundance of $52.7×10^4$ cells/L. *Karenia mikimotoi* took second place, with an abundance of $2.0×10^4$ cells/L. Other species with abundances higher than 100 cells/L were *G. spirale* (446 cells/L), *P. minimum* (226 cells/L), *S. trochoidea* (188 cells/L), *G. instriatum* (134 cells/L), and *Protoperidinium* spp. (105 cells/L). The abundance of diatoms in III-S2 was much lower, and *Thalassiosira* spp. was the dominant diatom species. *Skeletonema* spp. was only found in a few samples from subgroup III-S2 in the northern part of the study area.

Sample T42 was quite different from the rest of the samples collected from the CRE and adjacent waters. Only four taxa (*Prorocentrum* sp., *Coscinodiscus jonesianus*, *Nitzschia* sp. and *Diploneis* sp.) were identified in this sample, and the abundance of phytoplankton was extremely low (below 80 cell/L for every species).

Biodiversity indices, namely the Pielou evenness index, Shannon index and Margalef index, were also similar within groups, but exhibited clear differences among groups (Table 6).

SIMPER analysis of the species-by-sample matrix was used to determine the species representing each group. Table 7 displays the average similarity of the four groups and the typical species contributing to the average within-group similarity. In Groups I and II,

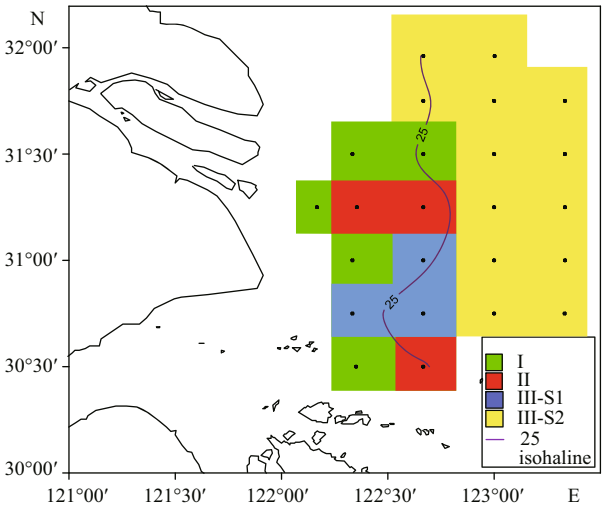

Fig.6 Horizontal distribution of phytoplankton groups in surface waters

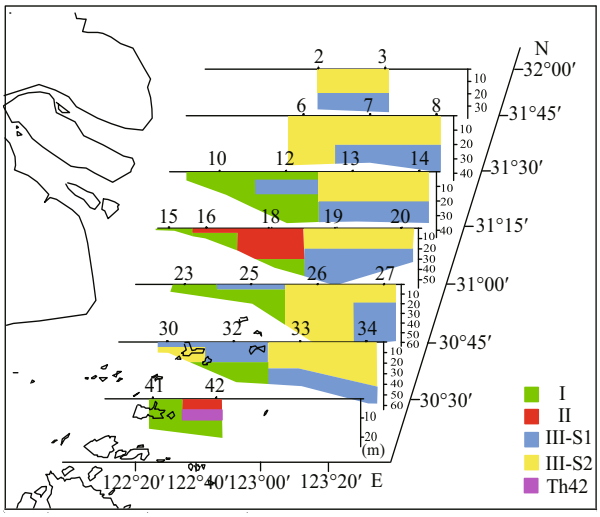

Fig.7 Vertical distribution of phytoplankton groups in different sections of the study area

Table 7 Typical species representing different groups, and their contributions (%) to the similarity within each group

Group		I	II	III	III-S1	III-S2
Average similarity		28.6	90.12	53.91	50.65	66.08
Contribution (100%)	*Prorocentrum donghaiense*	-	-	91.15	60.7	96.33
	Skeletonema sp.	26.9	98.61	-	-	-
	Paralia sulcata	27.14	-	-	26.92	-
	Thalassiosira sp.	20.48	-	-	4.61	-

the average similarities were 28.6% and 90.1%, respectively. In Group III, the average similarities were 50.7% and 66.1% for the two subgroups III-S1 and III-S2, respectively. *Skeletonema* sp., *P. donghaiense*, *Paralia sulcata* and *Thalassiosira* sp. were the most important species impacting similarities within each group.

3.4.3 Distribution patterns of different phytoplankton groups

Horizontal and vertical distribution patterns of the three groups of phytoplankton community are shown in Figs.6 and 7. Groups I and II were mainly distributed in the area west of 122°50′E. Group I was centered around the river mouth and the Shengsi islands, while Group II was situated around Group I. Group III was distributed further offshore compared with Groups I and II. Subgroup III-S1 was mainly found at the surface in the sea area north to the Shengsi islands and at the bottom east of 122°50′E. Subgroup III-S2 was mainly distributed at the surface, east of 122°50′E, but was also found west of 122°50′E in the northern part of the study area.

3.4.4 Environment factors associated with different groups

Environmental variables relating to the three phytoplankton groups are shown in Table 8. There were no apparent differences in seawater temperature among the groups, while salinity was significantly different among the groups. The salinities of Group I and II were 25.5 and 22.9, respectively, much lower than in Group III. The turbidity associated with the different groups also exhibited clear differences, with a gradual decrease from Group I to Group III. Highest turbidity was observed in Group I, with an average value of 327 NTU. The turbidity ranges associated with Group II (0.1–44.3) and Group III (0–39.8) were similar, but the average turbidity of Group II (23.4) was markedly higher than Group III.

4 DISCUSSION

In this study, discrete phytoplankton samples were collected from the sea area adjacent to the CRE during the outbreak stage of red tides in May 2009. Altogether, 94 taxa of microalgae were identified, including the most important red tide causative species in this region: *Skeletonema* spp., *P. donghaiense* and *K. mikimotoi*. Zou (2004) suggested a criterion for defining red tides of *Skeletonema costatum* (cell abundance higher than 5×10^7 cells/L). For other microalgal species, the criteria have been suggested as 10^6 cells/L or 3×10^5 cells/L for microalgae with cell sizes of 10–29 μm or 30–99 μm,

Table 8 The arithmetic mean and range (minimum-maximum) of the environment factors associated with different groups

	Temperature (°C)	Salinity	Turbidity (NTU)
I	17.8 (16.4–19.8)	25.5 (10.4–32.7)	327.0 (0.3–1820)
II	18.5 (16.6–19.8)	22.9 (7.9–32.7)	23.4 (0.1–44.3)
III	18.3 (16.7–21.1)	30.2 (19.1–33.5)	2.4 (0–39.8)
III -S1	17.4 (16.7–21.1)	31.0 (19.1–33.5)	5.5 (0–39.8)
III-S2	18.8 (16.8–20.1)	29.6 (23.8–33.5)	0.4 (0–9.78)
T42	17.40	28.32	53.01

respectively (Adachi, 1973). According to these criteria, four patches of red tides were found in the study area, formed by *Skeletonema* spp., *P. donghaiense* and *K. mikimotoi*. The *Skeletonema* spp. red tide occurred in the central part of the study area near sampling site 18. There were two red tide patches formed by *P. donghaiense*; one appeared in the sea area near sampling sites 2 and 3 in the northern part of the study area, and the other near sampling site 34 in the southern part of the study area. Another small red tide patch, formed by *K. mikimotoi*, was found near sampling site 19. Although *K. mikimotoi* had a relatively low cell density (maximum cell density at 3.5×10^5 cells/L), it was the second dominant species of dinoflagellates in the phytoplankton community and an important fish-killing species. Therefore, the red tide formed by *K. mikimotoi* should not be neglected.

These red tides could be well represented by the groups/subgroups deduced from the cluster analysis of the phytoplankton samples. Based on the data matrix of taxa composition and abundance established in this study, the phytoplankton assemblage in the sea area adjacent to the CRE were classified into three groups at a similarity level of 30%, and Group III could be further divided into two subgroups (III-S1, III-S2) at a similarity level of 40%. Group II represented *Skeletonema* spp. red tide, and Subgroup III-S2 represented dinoflagellate red tides of *P. donghaiense* and *K. mikimotoi*. Based on the distribution of different red tides, it can be seen that there was a gradual change in red tide causative species from the estuary to the offshore sea area, from diatoms to armored dinoflagellates and then unarmored dinoflagellates.

The CRE and its adjacent waters have a complex physical and chemical environment, affected by the Changjiang River diluted water, alongshore currents, and upwelling. Cluster analysis allowed us to relate the distribution of phytoplankton and red tides (as represented by different groups/subgroups) to environmental factors and processes, including salinity, turbidity, and upwelling.

4.1 Effects of temperature, salinity and turbidity

Based on the environmental data, water temperature in the study area (16.4–21.1°C) did not affect the distribution of phytoplankton and red tides. The maximum difference in temperature among the three phytoplankton groups was only 0.7°C. According to previous studies, the optimal temperature for the growth of *P. donghaiense* is 22–28°C (Deng et al., 2009), but the growth of *P. donghaiense* would not be significantly limited when water temperature was higher than 15°C (Wang et al., 2006). Similarly, the optimal temperature for the growth of *S. costatum* is 22°C (Xu et al., 2010), and its growth rate at 16°C is similar to the maximum growth rate at 22°C (Chen et al., 2005). Therefore, water temperature in the study area is not a limiting factor for the growth of these red-tide causative species, and will not affect the distribution of red tides.

Salinity, however, was an important factor affecting the distribution of phytoplankton and red tides in the CRE and adjacent waters. Phytoplankton communities in the central and western parts of the study area were characterized by estuarine diatoms dominated by *Skeletonema* spp. Previous studies suggested that the diatom *S. costatum* can adapt to a wide range of salinities, and the optimal salinity range was 18–25.7 (Chen et al., 2005). In this study, *Skeletonema* spp. could be observed in Groups I, II and Subgroup III-S1, with a wide salinity range. However, the optimal salinity range for the growth of *P. donghaiense* (25–31) was much narrower and higher than for the diatom *S. costatum* (Chen et al., 2005). Therefore, subgroup III-S2, which was characterized by the *P. donghaiense* red tide was found further offshore and had a higher salinity value of 29.6.

The impacts of salinity on the distribution of phytoplankton and red tides may reflect the potential role of nutrients. Unfortunately, nutrient data were not available in this study. In previous studies in this region, however, it was found that nutrient concentration has a negative linear correlation with salinity (for example, Huang et al., 1986). Therefore, a decreasing trend of nutrient concentrations from the estuary to the offshore area can be expected. This trend is likely to affect the distribution of red tides, since the diatom *Skeletonema* spp. and dinoflagellate

P. donghaiense have different nutrient utilization features. *Skeletonema costatum* can absorb nutrients rapidly (Wang et al., 2006), and the consensus is that diatoms grow much faster than dinoflagellates when there are enough nutrients available (Furnas, 1990). Therefore, red tides of *Skeletonema* spp. are often found in sea areas just outside the estuary, as observed in the current study. In the sea area further offshore, where nutrient concentration could limit the growth of diatoms, dinoflagellate *P. donghaiense* would have a greater opportunity to form red tides. This could account for the horizontal distribution patterns in red tides in the sea area adjacent to the CRE.

Turbidity was also a major limiting factor for the growth of phytoplankton in the estuary. In the CRE and adjacent waters, there was a negative relationship between turbidity and salinity. This is not unexpected, since both parameters are influenced by the Changjiang River runoff. The Changjiang River brings huge amounts of sand and silt into the East China Sea. The suspended materials will decrease the amount of photosynthetically active radiation entering the water. In the area near the estuary west of 122°E, the growth of phytoplankton is expected to be limited by light due to the high concentration of suspended substances (Shen, 1993). The horizontal gradient of suspended materials and a sediment front have been documented in the CRE and adjacent waters (Hu and Hu, 1995), influenced by the Changjiang plume and tide. *Skeletonema* spp. was the dominant species in both Groups I and II, but the average turbidity of Group II was only 24.3 NTU, much lower than that of Group I (327 NTU). The sharp decrease in turbidity seemed to be a major factor for the outbreak of the diatom red tide caused by *Skeletonema* spp. *Prorocentrum donghaiense* is adaptable to a wide range of illuminations (2–223 μmol/(m^2·s)) (Xu et al., 2010), and thus light itself is unlikely to explain the varying distribution of red tides caused by *Skeletonema* spp. and *P. donghaiense*.

4.2 Effects of physical oceanographic processes

Plume fronts, stratification and upwelling are important physical oceanographic phenomena and processes in the CRE and adjacent waters. A salinity value of 25 was often regarded as a convenient marker for the plume front, which can affect the biological, chemical and hydrological features of the estuary. The plume front zone, which has relatively low suspended matters and moderate nutrients for marine phytoplankton, has higher productivity (Hu and Hu, 1995). In this study, the 25-isohaline runs southwards from sites 2 to 32, fitting in well with the distribution of the diatom red tide (Group II) and dinoflagellate red tide (Subgroup III-S2).

Stratification and upwelling also appeared to play important roles in the distribution of phytoplankton communities. According to the vertical distribution of salinity (Fig.8), seawater from the open ocean with high salinity formed a wedge from the seabed towards the estuary. Affected by the bottom topography at sampling sites 23–27 and 30–34, upwelling formed from May to August in an area centered at 31°30′N and 122°40′E (Zhao, 1993). Strong upwelling at sampling site 32 resulted in low-temperature and high-salinity seawater at the surface, and the presence of abundant benthic diatom *P. sulcata*. During the investigation, *P. donghaiense* was not the dominant species at sampling site 32, probably due to the mixing effects caused by upwelling and relatively high concentration of nutrients (Bu et al., 2005). In the sea area nearby, where the effects of upwelling declined and stratification developed, the relatively stable condition allowed *P. donghaiense* to form a red tide (Group III-S2).

Considering the classification of phytoplankton assemblages and the effects of different environmental factors, it was suggested that phytoplankton Group I is closely associated with turbidity, Group II with turbidity, nutrients and plume front, subgroup III-S1 with upwelling and stratification, and subgroup III-S2 with salinity, nutrients and stratification.

5 CONCLUSION

(1) During an investigation in the sea area adjacent to the CRE in May 2009, water samples were collected and phytoplankton taxa composition and abundance were determined. Red tides of diatoms *Skeletonema* spp. and dinoflagellates *P. donghaiense* and *K. mikimotoi* were observed. The red tide of *Skeletonema* spp. appeared in the front zone of the Changjiang River plume, associated with low salinity and high nutrient availability. The red tide of *P. donghaiense* was distributed further offshore, outside the plume front zone, in the sea area with high salinity and low turbidity where stratification was well developed. The red tide of *K. mikimotoi* was observed in the sea area associated with high salinity and relatively low nutrient availability. The causative species of red tides exhibited a gradual change from the estuary to the offshore sea area, from diatoms to armored dinoflagellates and then unarmored dinoflagellates;

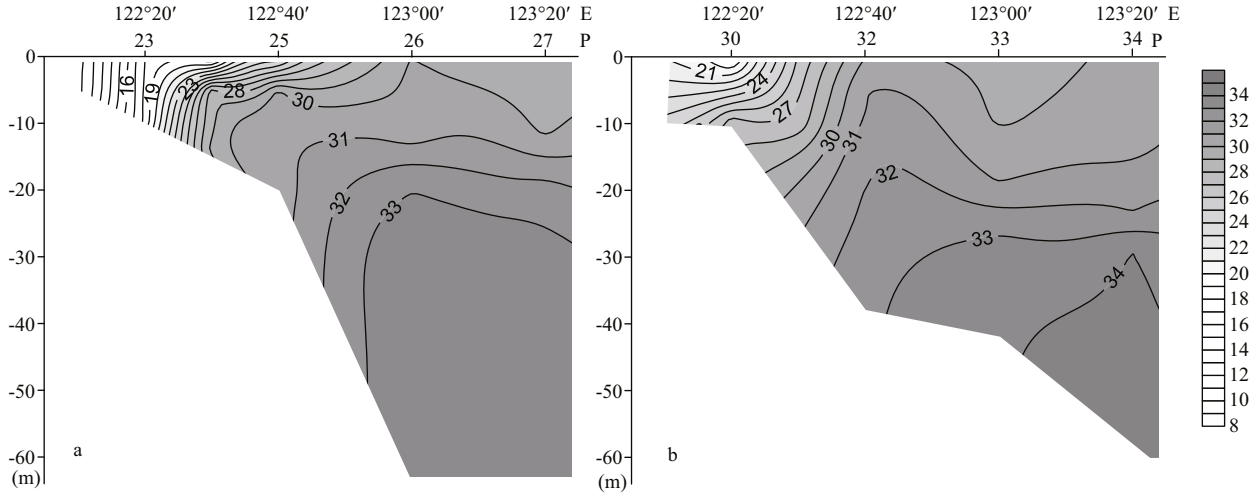

Fig.8 Vertical profiles of salinity in sections along sampling sites 23–27 (a) and 30–34 (b)

(2) A data matrix, including taxa composition and cell abundance of the phytoplankton samples, was established and used for non-metric multidimensional scaling, cluster analysis, and analysis of similarities (ANOSIM). Analyses categorized the samples into three groups (Group I, II, III) at the 30% similarity level. Group III could be further divided into two subgroups (III-S1, III-S2). Group II and subgroup III-S2 could represent the red tides of diatoms *Skeletonema* spp. and dinoflagellates *P. donghaiense* and *K. mikimotoi*;

(3) Salinity, turbidity, plume front, upwelling, stratification and (probably) nutrients were important factors affecting the distribution of phytoplankton and red tides in the sea area adjacent to the CRE. Group I was closely associated with turbidity, Group II with turbidity, nutrients and plume front, subgroup III-S1 with upwelling and stratification, and subgroup III-S2 with salinity, nutrients and stratification.

6 ACKNOWLEDGEMENT

The authors thank Dr. LI Yang of South China Normal University for his help in diatom identification and Dr. LIU Xiaoshou of Ocean University of China for his assistance with PRIMER analysis.

References

Adachi R. 1973. Organisms of red tide and actual situation of red tide. *Fisheries Engineering*, **9**(1): 31-36. (in Japanese)

Bu X W, Xu W Y, Zhu D D, Chen G X. 2005. Discussion about mechanism of harmful algal blooms breakout. *Acta Oceanol. Sin.*, **24**(1): 101-106.

Chen B Z, Wang Z L, Zhu M Y, Li R X. 2005. Effects of temperature and salinity on growth of *Prorocentrum dentatum* and comparisons between growths of *Prorocentrum dentatum* and *Skeletonema costatum*. *Advances in Marine Science*, **23**(1): 60-64. (in Chinese with English abstract)

Chen H L, Lv S H, Zhang C S, Zhou D D. 2006. A survey on the red tide of *Prorocentrum donghaiense* in East China Sea, 2004. *Ecologic Science*, **25**(3): 226-230. (in Chinese with English abstract)

Clarke K R, Gorley R N. 2006. PRIMER v6: User Manual/ Tutorial. PRIMER-E, Plymouth. 192p.

Clarke K R, Warwick R M. 2001. Change in Marine Communities: An Approach to Statistical Analysis and Interpretation. 2nd edn. PRIMER-E, Plymouth. 172p.

Deng G, Geng Y H, Hu H J, Qi Y Z, Lv S H, Li Z K, Li Y G. 2009. Effects of environmental factors on photosynthesis of a high biomass bloom forming species *Prorocentrum donghaiense*. *Marine Sciences*, **33**(12): 34-39. (in Chinese with English abstract)

Furnas M J. 1990. *In situ* growth rates of marine phytoplankton: approaches to measurement, community and species growth rates. *J. Plankton Res.*, **12**(6): 1 117-1 151.

Gao X L, Song J M. 2005. Phytoplankton distributions and their relationship with the environment in the Changjiang Estuary, China. *Mar. Pollut. Bull.*, **50**(3): 327-335.

GEOHAB. 2001. Global ecology and oceanography of harmful algal blooms, science plan. *In*: Glibert P, Pitcher G eds. SCOR and IOC. Baltimore and Paris. 87p.

Guo Y J, Yang Z Y. 1992. Quantitative variation and ecological analysis of phytoplankton in the estuarine area of the Changjiang River. *Studia Marina Sinica*, **33**: 168-189. (in Chinese)

He Q, Sun J, Luan Q S, Yu Z M. 2009. Phytoplankton in Changjiang Estuary and adjacent waters in winter. *Marine Environmental Science*, **28**(4): 360-365. (in Chinese with English abstract)

Hu H, Hu F X. 1995. Water types and frontal surface in the Changjiang estuary. *Journal of Fishery Sciences of China*, **2**(1): 81-90. (in Chinese with English Abstract)

Huang S G, Yang J D, Ji W D, Yang X L, Chen G X. 1986. Spatial and temporal variation of reactive Si, N, P and their relationship in the Chang Jiang estuary water. *Journal of Oceanography in Taiwan Strait*, **5**(2): 114-123. (in Chinese with English Abstract)

Huang X Q, Jiang X S, Tao R, Hong J C. 2000. Multi-variate analysis of the occurring process of *Skeletonema costatum* red in Changjiang Estuary. *Marine Environmental Science*, **19**(4): 1-5. (in Chinese with English abstract)

Kong F Z, Yu R C, Xu Z J, Zhou M J. 2012. Application of excel in calculation of biodiversity indices. *Marine Sciences*, **36**(4): 57-62. (in Chinese with English abstract)

Luan Q S, Sun J, Shen Z L, Song S Q, Wang M. 2006. Phytoplankton assemblage of Yangtze River Estuary and the adjacent east China sea in summer, 2004. *Journal of Ocean University of China*, **5**(2): 123-131.

Lund J W G, Kipling C, Le Cren E D. 1958. The inverted microscope method of estimating algal numbers and the statistical basis of estimations by counting. *Hydrobiology*, **11**(2): 143-170.

Margalef R. 1958. Information theory in ecology. *General Systematics*, **3**: 36-71.

McNaughton S J. 1967. Relationships among functional properties of California grassland. *Nature*, **216**(5111): 168-169.

Pei S F, Shen Z L, Laws E A. 2009. Nutrient dynamics in the upwelling area of Changjiang (Yangtze River) estuary. *J. Coastal Res.*, **25**(3): 569-580.

Pielou E C. 1966. The measurement of diversity in different types of biological collections. *J. Theor. Biol.*, **13**: 131-144.

Shannon C E. 1948. A mathematical theory of communication. *Bell System Technical Journal*, **27**(3): 379-423.

Shen H, Hong J C. 1994. Investigation report on the *Skeletonema costatum* red tide in Changjiang River estuary-study on the phytoplankton community composition and cell morphology. *Oceanologia et Limnologia Sinica*, **25**(6): 591-595. (in Chinese with English abstract)

Shen Z L. 1993. The effects of the physic-chemical environment on the primary productivity in the Yangtze River estuary. *Transactions of Oceanology and Limnology*, (1): 47-51. (in Chinese with English abstract)

Sun J, Tian W. 2011. Phytoplankton in Yangtze River estuary and its adjacent waters in spring in 2009: species composition and size-fractionated chlorophyll *a*. *Chinese Journal of Applied Ecology*, **22**(1): 235-242. (in Chinese with English abstract)

Tang D L, Di B P, Wei G F, Ni I H, Oh I S, Wang S F. 2006. Spatial, seasonal and species variations of harmful algal blooms in the South Yellow Sea and East China Sea. *Hydrobiologia*, **568**(1): 245-253.

Utermöhl H. 1958. Zur Vervolkommung der quantitativen Phytoplankton—Methodik. *Mit. Int Ver Theor Angew Limnol.*, **9**: 1-38. (in German)

Wang B D, Zhan R, Zang J Y. 2002. Distributions and transportation of nutrients in Changjiang River Estuary and its adjacent sea areas. *Acta Oceanol. Sin.*, **24**(1): 53-58. (in Chinese with English abstract)

Wang B D. 2007. Assessment of trophic status in Changjiang (Yangtze) River estuary. *Chin. J. Oceanol. Limnol.*, **25**(3): 261-269.

Wang J H, Huang X Q. 2003. Ecological characteristics of *Prorocentrum dentatum* and the cause of harmful algal bloom formation in China sea. *Chinese Journal of Applied Ecology*, **14**(7): 1 065-1 069. (in Chinese with English abstract)

Wang J H. 2002. Phytoplankton communities in three distinct ecotypes of the Changjiang Estuary. *Journal of Ocean University of Qingdao*, **32**(3): 422-428. (in Chinese with English abstract)

Wang Z L, Li R X, Zhu M Y, Chen B Z, Hao Y J. 2006. Study on population growth processes and interspecific competition of *Prorocentrum donghaiense* and *Skeletonema costatum* in semi-continuous dilution experiments. *Advances in Marine Science*, **24**(4): 495-503. (in Chinese with English abstract)

Wu Y L, Zhang Y S, Zhou C X. 2000. Phytoplankton distribution and community structure in the East China Sea (ECS) continental shelf. *Chin. J. Oceanol. Limnol.*, **18**(1): 74-79.

Xu N, Duan S S, Li A F, Zhang C W, Cai Z P, Hu Z X. 2010. Effects of temperature, salinity and irradiance on the growth of the harmful dinoflagellate *Prorocentrum donghaiense* Lu. *Harmful Algae*, **9**(1): 13-17.

Zhao B R. 1993. Upwelling outside of Changjiang River estuary. *Acta Oceanologica Sinica*, **15**(2): 108-114. (in Chinese with English abstract)

Zhao R, Sun J, Bai J. 2010. Phytoplankton assemblages in Yangtze River estuary and its adjacent water in autumn, 2006. *Maine Sciences*, **34**(4): 32-39. (in Chinese with English abstract)

Zhou M J, Shen Z L, Yu R C. 2008. Responses of a coastal phytoplankton community to increased nutrient input from the Changjiang (Yangtze) River. *Cont. Shelf Res.*, **28**(12): 1 483-1 489.

Zhou M J, Yan T, Zou J Z. 2003. Preliminary analysis of the characteristics of red tide areas in Changjiang River estuary and its adjacent sea. *Chinese Journal of Applied Ecology*, **14**(7): 1 031-1 038. (in Chinese with English abstract)

Zhou M J, Yu R C. 2007. Mechanisms and impacts of harmful algal blooms and the countmeasures. *Chinese Journal of Nature*, **29**(2): 72-77. (in Chinese with English abstract)

Zhou M J, Zhu M Y. 2006. Progress of the project "Ecology and Oceanography of Harmful Algal Blooms in China". *Advances in Earth Science*, **21**(7): 673-679. (in Chinese with English abstract)

Zou J Z. 2004. Marine Environmental Science. Shandong Education Press, Jinan, China. p.258-259. (in Chinese)